Design, Manufacture and Test of the Superconducting Quadrupole Triplet Magnet with Multi-layered Direct-wound Hexapole and Octupole Magnets

Junseong Kim, Dongkeun Park, Seokho Nam, Chang-Geun Yang, Young Gon Kim, Sukjin Choi, Do Gyun Kim, Hyun Man Jang, and Seungje Lee

***Abstract*—Currently, the Rare Isotope Science Project of the Institute for Basic Science has been constructing a heavy ion accelerator facility, named RAON. For rare isotope science research in Korea, the RAON includes two different types of facilities; one is the isotope separation on-line, and another is the in-flight system. In the in-flight system, several types of magnets are located: dipole, quadrupole, hexapole, and octupole magnets. Among them, a superconducting quadrupole triplet magnet (SQTM) system has been developed since 2018 and to date, all SQTM systems were manufactured and are being tested. In this paper, the design, manufacture, and commissioning test results of the SQTM systems for the RAON are presented. This magnet consists of five magnets of three different kinds: three quadrupole magnets, a hexapole magnet, and an octupole magnet. All magnets were made by low-temperature superconducting NbTi wires. For manufacturing the hexapole and octupole magnets with a multi-layer structure in a narrow space, the low-temperature superconducting wire was wound by the direct winding method.**

***Index Terms*—accelerator, direct winding, RAON, superconducting quadrupole/hexapole/octupole magnet.**

I. Introduction

INSTITUTE for Basic Science (IBS) is now constructing a heavy ion accelerator complex, named Rare isotope Accelerator complexes for ON-line experiments (RAON) in Korea. The RAON is under construction as the first and optimal facility to generate new rare isotopes by combining two rare isotope production methods; isotope separation on-line and In-flight Fragmentation (IF) system [1], [2]. In the IF system, different types of superconducting magnets such as dipole, quadrupole, hexapole, and octupole magnets are used. Among these magnets, 13 units of the superconducting quadrupole triplet magnet (SQTM) have been developed by IBS and JH Engineering Ltd in Korea since 2018. Configuration of the IF system and 13 SQTMs are as shown in Fig. 1(a) [3], [4].

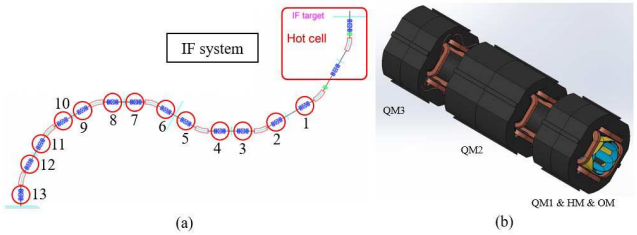

Fig. 1. (a) Magnets of the IF system and (b) configuration of superconducting quadrupole triplet magnet

To date the manufacture of all magnets has been completed and the experiments for verifying the performance of the magnet are being conducted. As shown in Fig. 1(b), A SQTM consists of three quadrupole magnets (QMs: QM1, QM2, and QM3), one hexapole magnet (HM), and one octupole magnet (OM). The HM and OM are each designed as a 4-layered coil and using the direct winding method. All magnets are made using low-temperature superconducting (LTS) NbTi wires.

II. Design of the SQTM

A. QM Design with an Iron Yoke and NbTi Coils

A design of an iron yoke in the SQTM is crucial for creating a proper focusing or defocusing magnetic field as the iron yoke more generates a magnetic field than the superconducting coils [5]. As the first step of the iron yoke design, the 0.5-mm thick iron sheets which are PN-core made by POSCO Co., Ltd. were selected. We measured the B-H characteristic of the iron at different temperatures as shown in Fig. 2. Based on this B-H characteristic and magnetic field harmonics coefficients (HCs), the inner surface shape of the iron yoke was designed using (1) to generate the magnetic field shape suitable for the focusing/defocusing purpose of the QMs [6]-[8].

$$y = \pm \frac{r_{pole}^{\,2}}{2x} \tag{1}$$

This work was supported by the Technological Innovation R&D Program (S2955267) funded by the Ministry of SMEs and Startups (MSS, Korea)
(Corresponding author: Seungje Lee)

Junseong Kim was with the JH Engineering Corporation Ltd., Anyang-si 14119, South Korea. He is now with the Plasma Science and Fusion Center, MIT, Cambridge, MA 02139 USA. (e-mail: junseong@mit.edu)

Dongkeun Park is with the Plasma Science and Fusion Center, MIT, Cambridge, MA 02139 USA.

Seockho Nam was with the JH Engineering Corporation Ltd., Anyang-si 14119, South Korea. He is now with the Korea Institute of Fusion Energy, Daejeon 34133, Korea

Chang-Geun Yang, Young Gon Kim, and Seungje Lee is with the JH Engineering Corporation Ltd., Anyang-si 14119, South Korea. (e-mail: sjlee@thinkers.co.kr)

Sukjin Choi, Do Gyun Kim, Hyun Man Jang is with the Rare Isotope Science Project, Institute for Basic Science, Daejeon 34047, South Korea.

Template version 8.0d, 22 August 2017. IEEE will put copyright information in this area
See http://www.ieee.org/publications_standards/publications/rights/index.html for more information.

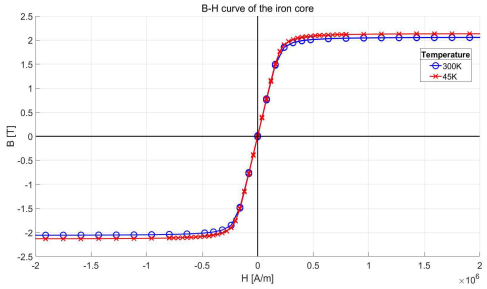

Fig. 2. Measured B-H curve of the selected iron sheet at 300K and 45K.

where r_{pole} is the pole tip radius of 180 mm for the QM1 (170 mm for the QM2 and QM3), x and y are the iron yoke surface positions. The magnetic field of a quadruple magnet is represented by HCs in cylindrical coordinates under the condition of free space without current sources or sinks [9]. The QM1 has a larger pole tip radius because the HM and OM are placed inside the magnet. The cross-section view of the iron yoke and magnetization of the initially designed iron yoke is shown in Fig. 3(a). Here, the magnetization of the iron yoke pole is not uniform. For making more uniform magnetization near the inner surface, the saturation control hole (SCH) method was applied to the iron yoke design as shown in Fig. 3(b). The more the iron yoke magnetized uniformly, the more saturation-induced harmonics can be reduced [10], [11].

The racetrack-shaped NbTi coil was designed to generate the required magnetic field for the QMs together with the iron yoke. Table I shows the detailed properties of NbTi wire and the designed specification of the iron yoke and racetrack-shaped coil for the QM. The 1600-turn NbTi racetrack coils

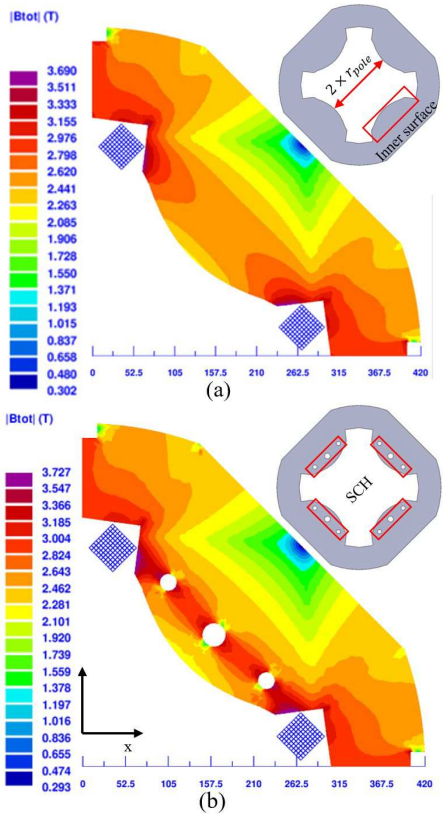

Fig. 3. Magnetization of the iron yoke (a) without SCH and (b) with SCH.

TABLE I
SPECIFICATION OF THE QUADRUPOLE MAGNETS

Physical Property	QM1	QM2	QM3
LTS wire material		NbTi	
Bare diameter		1.02 mm	
Insulated dimeter		1.10 mm	
Cu/NbTi ratio		4.3	
RRR		> 120	
Breakdown voltage		2000 V	
Critical current		at 4.2K, and $10^{-14}\Omega$·m	
at 3T		685 A	
at 4T		570 A	
Total length per coil	~2.8 km	~3.9 km	~2.8 km
Iron yoke material		Non grain-oriented electrical steel	
Length	450 mm	800 mm	450 mm
Pole tip radius, r_{pole}	180 mm	170 mm	170 mm
Outer radius		420 mm	
LTS coil		Racetrack shape	
Cross section, T_{coil}		44 mm x 44 mm	
Long straight length, L_{coil}	450 mm	800 mm	450 mm
Short straight length, sL_{coil}		368.9 mm	
Radius, R_{coil}		50 mm	
Field gradient		≥ 11 T/m	
Maximum operating current	150 A	140 A	140 A
Maximum field at coil		3.6 T	

with a cross-sectional area of 44 mm x 44 mm was designed to meet the specification as shown in Fig. 4(a). Considering the interference between the additional support, the iron yoke was symmetrically trimmed except inner surface as shown in Fig. 4(b). The quench analysis simulation for all magnets was performed in a previous study [12].

B. *Design of Direct-wound HM and OM*

As shown in Fig. 1b, the HM and OM are placed inside the QM1 of which the pole tip radius is 10 mm larger than that of QM2 and QM3. To be placed in this limited radial space with our designed shape and generate the required magnetic field, the HM and OM were designed to be wound with the direct winding method [13]-[15]. Furthermore, by this serpentine shape, the number of superconducting junctions and the mag-

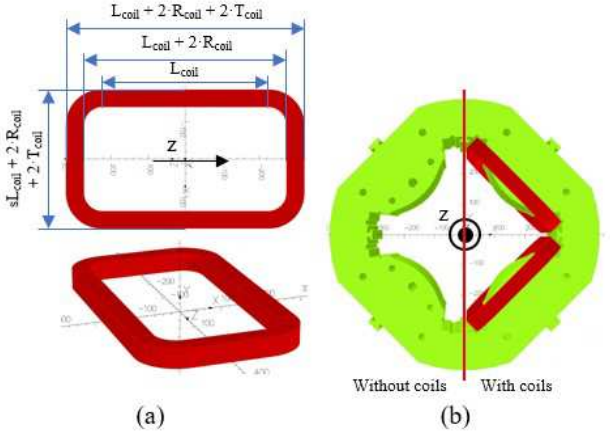

Fig. 4. Designed LTS racetrack coil and iron yoke with the coil.

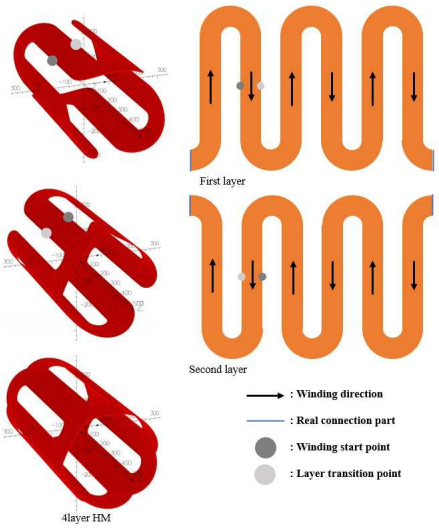

Fig. 5. A direct winding method applying for the hexapole magnet.

(a) (b) (c)

Fig. 6. Photos of (a) an impregnated NbTi racetrack coil, (b) an iron sheet for the QM yoke, and (c) a stacked iron yoke.

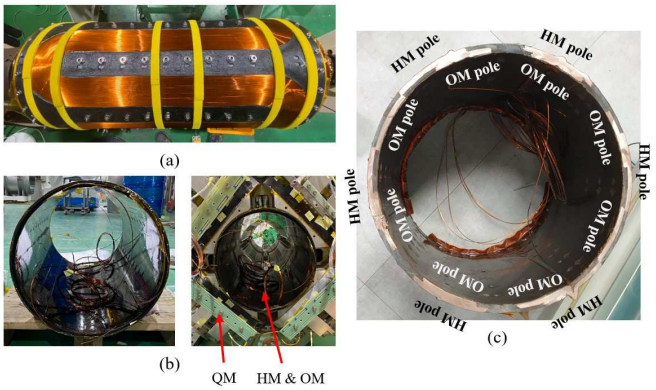

Fig. 7. Photos of (a) making progress of the direct winding magnet, and (b) a manufactured and assembled with QM of one-body HM and OM. (c) Cross sectional picture of the production failed HM and OM

netic field effect of the coil end can be reduced.

The principle of the direct winding method is described in Fig. 5. The direct winding starts from the winding start point and ends at the layer transition point. When winding is completed at a layer transition point, it can transition to the next layer, then, next layer winding starts at the point again. In this way, after completing the winding at the transition point in the first layer, only the thickness of the layer is moved in the radial direction, and the winding of the second layer is started again. And the transition point which is the winding end point of the second layer is a position moved by the thickness of the layer only in the radial direction from the winding start point of the first layer. In this way, many layers of the HM and OM were fabricated.

TABLE II
SPECIFICATION OF HM AND OM

Physical Property	HM	OM
LTS wire	NbTi	
Number of straight part (pole)	6	8
Inner radius	175 mm	170 mm
Outer radius	180 mm	175 mm
Turns in a layer	90	65
Number of layers	4	4
Straight length	397 mm	460 mm
Total length of wire	~2.3 km	~ 1.9 km

The straight part of the layers is wound in the same direction, curve parts of the layers are not overlapped completely, but it is wound slightly overlapping. Using the 1.1 mm ϕ NbTi wire, same as used in QMs, with the direct winding method, the HM and OM, each has 4 layers, i.e., a total 8-layers, were designed to be placed in a space of 10mm. The HM and OM are designed to be manufactured as an one body structure using prepreg. The designed specifications of HM and OM are summarized in Table II.

III. MANUFACTURE OF SQTM

The NbTi racetrack coils and iron yokes for the QMs were fabricated. Fig. 6(a) shows the epoxy impregnated NbTi racetrack coil removed from the winding bobbin. The NbTi coils were wound orthocyclically and automatically by a robotic arm machine on the specially designed aluminum winding bobbin, and then treated epoxy vacuum pressure impregnation. After the epoxy was fully cured, we removed the winding bobbin. The iron yoke was manufactured by stacking 0.5 mm thickness iron sheets which were cut as designed by laser machine with a 98% lamination factor. Fig. 6(b) shows a single iron sheet showing designed pattern. The QM is combined by 4 impregnated NbTi coils and a stacked iron sheet as shown in Fig. 6(c). The eddy current loss in the iron yoke can be reduced by laminating.

The OM was wound with the same type NbTi in Table I and then, the HM was wound, both by using the direct winding method, on top of the OM to form a one-body shape to minimize a radial build. Epoxy prepreg sheets were inserted between layers and two magnets. Fig. 7(a) shows the directing winding process for the outer HM. After completion of winding, this direct-wound magnets were cured and then, the winding bobbin was removed. A completed one-body shaped HM and OM is shown in Fig. 7(b). Although the magnet was manufactured incorrectly during the heat cure process as shown in Fig. 7(c), the picture shows that the OM and HM were properly wound with the direct winding method into our designed one-body shape.

The assembling process of the SQTM is presented in Fig. 8. The QM1 with the one-body HM and OM inside, QM2 and QM3 were assembled as shown in Fig. 7(b) and 8a. Then, this

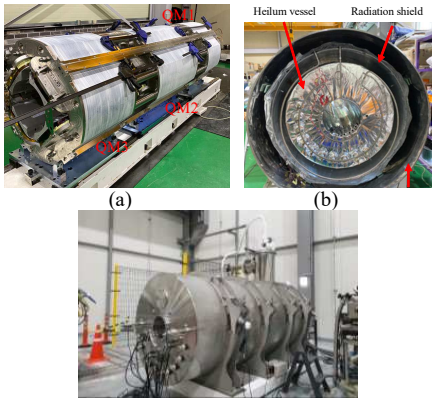

Fig. 8. Photos of (a) the manufactured quadrupole triplet magnet, (b) LHe vessel(with magnet), radiation shield and vacuum vessel, and (c) the SQMT.

Fig. 9. A photo of the mapping system for the SQTM.

combined magnet was inserted in the cryostat. Figure 8(b) shows a front view of cryostat before closing the front end flanges. The magnet, helium vessel, radiation shield, and vacuum vessel were placed and suspended concentrically. The final completed SQTM is shown in Fig. 8(c).

IV. Magnetic Field Test

The experiment was conducted to verify the magnetic field performance of the manufactured SQTMs. The SQTM was cooled by liquid helium and tested at 4.2 K. The magnetic field distribution was measured along a circular path, which radius is 110 mm and angular positions are from 0 to 355 degrees by 5 degrees intervals, xy-planes along the z-axis, which z-mapping points are from 0 mm to 3200 mm by 10 mm interval, by the mapping system as shown in Fig. 9. A hall probe with high-precision and low-noise performance made by SENIS in the mapping system was used for precisely measuring the magnetic field.

Based on the measured magnet field that was measured at the 110 mm radius circle along the beam axis, HCs and magnetic field gradient were calculated. First, the change of gradient strength as the operating current increases is shown in Fig. 10. The gradient of QMs (Fig. 10(a)), the iron-dominated magnet, changes similarly with the magnetic field saturation curve of iron as the operating current increases. On the other hand, the magnetic field gradient of the HM and OM which are placed inside the iron yoke and generate small magnetic fields are linear according to the operating current.

In Fig. 11, the main field HC of each magnet is represented according to the z-axis position. The main HC of QMs, HM, and OM are the 4pole, 6pole, and 8pole, respectively. The

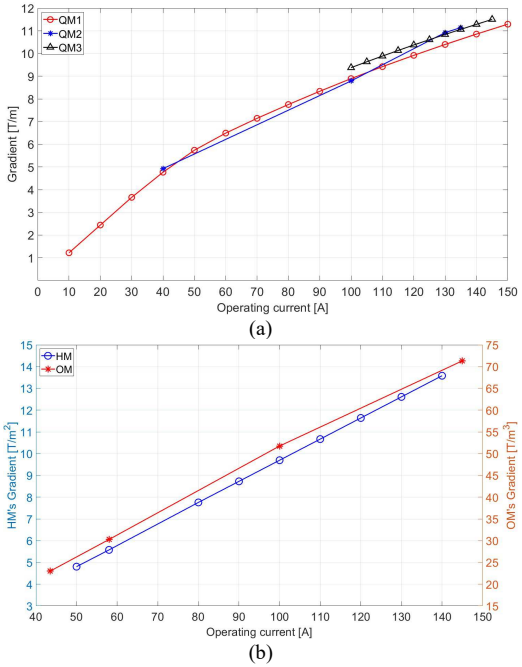

Fig. 10. Measured field gradient strength as a function of the operating current:. (a) the QM1, QM2, and QM3; and (b) HM, and OM.

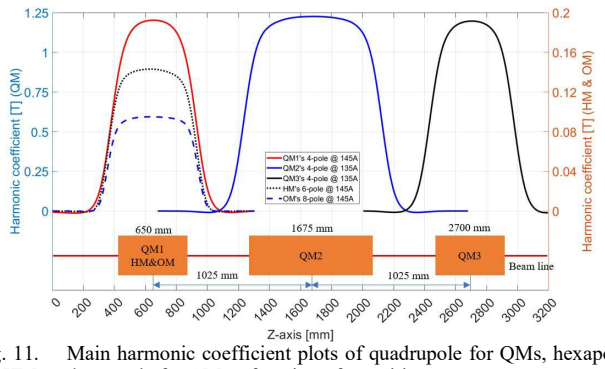

Fig. 11. Main harmonic coefficient plots of quadrupole for QMs, hexapole for HM, and octupole for OM as function of z position.

main HC changes along the z-axis of each QM are within the designed range. The proper shape of the main HC of the HM and OM was sufficient to validate our manufacturing of the SQTM and the direct winding method.

V. Conclusion

JH Engineering Ltd. and IBS have successfully developed the superconducting quadrupole triplet magnet for RAON, a heavy-ion accelerator.

A total 13 units of SQTMs were manufactured and tested to verify their performance. SQTMs successfully reached the target operating current up to 150 A after a few pre-training quenches and the magnetic field distributions were measured to compute gradients and the HCs of the QMs, HM and OM. The gradients and main HCs of SQTMs were properly generated showing the magnitudes and shapes as designed. Based on the field mapping results, we have validated our manufacturing process of the SQTM including the direct winding technique we applied for the HM and OM.

REFERENCES

[1] Jeon, D., Hong, I. S., Kim, H. J., Kim, J. W., Bodenstein, R. M., Cha, H. J., Choi, S. J., Choi, S., Choi, O. R., Do, H., Choi, B. H., Choi, C. J., Han, J., Han, W. K., Hyun, M. O., Jang, H., Joo, J. D., Joung, M. J., Jung, H. C., … Kim, E. S. (2014). Design of the RAON accelerator systems. *Journal of the Korean Physical Society*, *65*(7), 1010–1019. https://doi.org/10.3938/jkps.65.1010

[2] Kim, Young Jin. "Current status of experimental facilities at RAON." *Nuclear Instruments and Methods in Physics Research Section B: Beam Interactions with Materials and Atoms* 463 (2020): 408-414.

[3] Kim, D. G., et al. "Magnet designs of the in-flight fragment separator for the RISP." *presented at the Int. Particle Accelerator Conf. 2013*. 2013.

[4] Jo, Hyun Chul, et al. "Prototype HTS quadrupole magnet for the in-flight fragment separator of RISP." *IEEE Transactions on Applied Superconductivity* 28.6 (2018): 1-6.

[5] Zhang, Zhan, et al. "A study on the optimization of an HTS quadrupole magnet system for a heavy ion accelerator through evolution strategy." *IEEE transactions on applied superconductivity* 26.4 (2016): 1-4.

[6] Chernosvitov, Alexander, Alexander Kalimov, and Hermann Wollnik. "Design of an iron dominated quadrupole magnet with a high pole-tip flux density." *IEEE transactions on applied superconductivity* 12.1 (2002): 1430-1433.

[7] Hillert, Wolfgang. "Transverse linear beam dynamics." *arXiv preprint arXiv:2107.02614* (2021).

[8] Jain, Animesh K. "Harmonic coils." (1998).

[9] J. Kim *et al*., "Experimental Test of the Magnetic Field Active Shimming Method for Air-Core HTS Quadruple Magnet," in *IEEE Transactions on Applied Superconductivity*, vol. 30, no. 4, pp. 1-5, June 2020, Art no. 4600805, doi: 10.1109/TASC.2020.2966462.

[10] Gupta, R., et al. *FIELD QUALITY IMPROVEMENTS IN SUPERCONDUCTING MAGNETS FOR RHIC*. No. BNL-68135; KA0403011. Brookhaven National Lab.(BNL), Upton, NY (United States), 1994.

[11] Gupta, R., et al. "Field quality control through the production phase of RHIC arc dipoles." *Proceedings Particle Accelerator Conference*. Vol. 3. IEEE, 1995.

[12] Lee, Wooseung, et al. "Quench Analysis of an LTS Quadrupole Triplet Magnet System for the IBS RAON In-Flight Fragment Separator." *IEEE Transactions on Applied Superconductivity* 30.4 (2020): 1-4.

[13] Parker, Brett, et al. "BNL direct wind superconducting magnets." *IEEE transactions on applied superconductivity* 22.3 (2011): 4101604-4101604.

[14] Gupta, Ramesh. "Optimum integral design for maximizing the field in short magnets." *IEEE transactions on applied superconductivity* 15.2 (2005): 1152-1155.

[15] Parker, Brett, and John Escallier. "Serpentine coil topology for BNL direct wind superconducting magnets." *Proceedings of the 2005 Particle Accelerator Conference*. IEEE, 2005.